THESIS FOR THE DEGREE OF DOCTOR OF PHILOSOPHY (Ph.D.)

Role of poly(ADP-ribose) polymerase-1 (PARP-1) and poly(ADP-ribose) glycohydrolase (PARG) in the regulation of cell death and in the expression of inflammatory mediators

by Katalin Erdélyi

Supervisor:
Dr. László Virág

UNIVERSITY OF DEBRECEN
DOCTORAL SCHOOL OF MOLECULAR MEDICINE

DEBRECEN, 2009

Supervisor:

Head of the Examination Committee:

Members of the Examination Committee:

The Examination takes place at

Medical and Health Science Center, University of Debrecen
, 2009

Head of the Defense Committee:

Reviewers:

Members of the Defense Committee:

The Ph.D. Defense takes place at
The Lecture Hall of 1st Department of Medicine,
Institute for Internal Medicine, Medical and Health Science Center, University of Debrecen
, 2009

1. INTRODUCTION

1.1 Poly(ADP-ribose) metabolism

Poly(ADP-ribosyl)ation is a reversible post-translational protein modification implicated in the regulation of a number of biological functions such as maintenance of genomic stability, transcriptional regulation, energy metabolism, centromere function, telomere dynamics, mitotic spindle formation during cell division and cell death. It occurs in almost all nucleated cells of mammals, plants and lower eukaryotes, but is absent in yeast.

PARP-1 is a nuclear enzyme activated by DNA break. Activated PARP-1 catalyses the formation of ADP-ribose from NAD^+ by cleavage of the glycosidic bond between nicotinamide and ribose. Subsequently PARP-1 mono(ADP-ribosyl)ate the glutamate, aspartate and carboxyterminal lysine residues of the acceptor protein, than catalyses an elongation and branching reaction using additional ADP-ribose units from NAD^+. This generates novel ribosyl-ribosyl linkage and eventually results in the formation of polymers with chain lengths of approximately 200 ADP-ribose units. The average branching frequency of the polymer is approximately one branch per linear section of 20-50 units of ADPr.

More then 30 nuclear substrates of PARPs have been identified: histones, DNA ligases, DNA polymerases, DNA topoisomerases, DNA dependent protein kinases, transcription factors, DNA repair proteins. The most prominent target protein (acceptor) of this poly(ADP-ribosyl)ation reaction is PARP-1 itself. Poly(ADP-ribose) polymers are covalently attached to the automodification domain which leads to the enzymatic inactivation of the PARP and also the release from the DNA

Poly(ADP-ribosylation) is transient and reversible. The degradation of poly(ADP-ribose) is catalyzed by poly(ADP-ribose) glycohydrolase (PARG) which has both exoglycosidase and endoglycosidase activities that hydrolyze the glycoside linkage between the ADP-ribose units producing free ADP-ribose. Remaining protein-proximal ADP-ribose monomers are removed by ADP-ribosyl protein lyase.

1.2 Cellular function of PARG

To elucidate the cellular function of PARG, pharmacological inhibition of the enzyme appeared to be a viable approach. In the 90th and the early 2000, years several in vitro studies suggested that tannins (gallotannin, ellagitannin or tannic acid), could be potent inhibitors of PARG. Tannic acids are naturally occurring water-soluble polyphenol compounds which primarily consist of a glucose core esterified with gallic acid or its derivative. These potent

inhibitors provided cytoprotection in two PARP-mediated cytotoxicity systems: N-methyl-D-aspartate (NMDA)-stimulated neurons and oxidatively stressed HaCaT cells. Moreover, it has been shown that these tannins lead to accumulation of poly(ADP-ribose).

Gallotannin and other tannins also have been shown to exert various biological effects ranging from anti-inflammatory to anticancer and antiviral effects. The mechanism underlying the anti-inflammatory effect of tannins include the scavenging of radicals (antioxidant effect) and inhibition of the expression of inflammatory mediators, such as cytokines, inducible nitric-oxide synthase and cyclooxygenase-2. Most of these studies focused on the effects of tannins on immune cells with special regard to mononuclear cells and macrophages. Despite of all of these beneficial effects of tannins, the lack of specificity limits their use in cell-based studies.

1.3. The diverse biological function of poly(ADP-ribosyl)ation

1.3.1. PARP-1 and PARG in DNA repair

A plethora of studies have firmly established that poly(ADP-ribosyl)ation significantly contributes to cellular recovery from cytotoxicity in proliferating cells inflicted with low or moderate levels of DNA damage establishing PARP-1 as a survival factor.

Single-strand breaks (SSB) are one of the most frequent DNA lesions produced by endogen reactive oxygen species or generated by oxidative agents or ionizing radiation. SSB are also intermediate products in various aspects of DNA metabolism, including DNA repair, replication and recombination. During base excision repait (BER) SSB are produced by DNA glycosylases and apuronic/apyrimidinic (AP) endonucleases at the site of base damage. Following the detection of single-strand-DNA breaks (SSBs) by PARP-1 and PARP-2, poly(ADP-ribose) synthesis at the DNA damage site triggers both the recruitment of the SSB-repair scaffold protein XRCC1 and the relaxation of the chromatin superstructure as mediated by the poly(ADP-ribosyl)ation of histone H1 and histone H2B tails. Together this facilitates access to the DNA lesion of repair enzymes that interact with XRCC1.

The importance of PARG for SSB-repair and cell survival remains to be elicited. It has been reported that PARG interacts with XRCC1 and that mice lacking PARG exhibit sensitivity to alkylating agents and γ-irradiation. However, it has also been reported that depletion of PARG protects mouse embryonic fibroblast (MEF) cells from hydrogen peroxide induced cell death and that PARG is dispensable for SSB-repair after oxidative stress.

1.3.2. PARP-1 and cell death

Cell death by necrosis occurs as a consequence of acute, excessive exposure to a pathological insult. It is characterized by cell swelling followed by disruption of cell membranes leading to the release of the cellular content in the environment, leading to inflammation of surrounding tissues. Apoptosis, also called programmed cell death, is a mechanism by which a cell commits to suicide in response to different stimuli like DNA damage, signals from neighboring cells, or extracellular chemical signals. In apoptotic cell death, cellular content is separated into vesicles that are engulfed by macrophages with little or no detrimental consequences for neighboring cells. In contrast to necrosis, apoptosis is an energy-dependent process that is generally executed by caspases (**c**ysteine-**asp**artic acid prote**ase**s), proteases activated to cleave specific substrates in order to inactivate cellular processes.

Interestingly, PARP-1 is inactivated during the execution phase of apoptosis. PARP-1 is cleaved by caspase-3 and -7 into two fragments eliminating its activation in response to DNA fragmentation during apoptosis and protecting the cells from ATP depletion and subsequent necrotic death. In addition, by preventing futile attempts at DNA repair, PARP-1 cleavage may help to commit cells to the apoptotic pathway.

Mitochondria play an amplification role in many apoptotic models and can also release factors involved in caspase-independent cell death including apoptosis-inducing factor (AIF). Nascent AIF has a mitochondrial localization sequence that is cleaved upon entry into the intermembrane space. In healthy cells, AIF is retained in the mitochondria where it is believed to perform an oxidoreductase function. However, upon certain stimuli, AIF translocates to the nucleus and initiates large scale (50kb) DNA fragmentation and chromatin condensation by recruiting or activating endonucleases. The translocation of AIF into the nucleus is impaired in PARP-$1^{-/-}$ fibroblasts after treatment with DNA-alkylating agent N-methyl-N-nitro-N-nitrosoguanidine (MNNG) that potently activates PARP-1. Exactly how PARP-1 activation triggers the release of AIF from mitochondria is not clear, however a product of poly(ADP-ribose) metabolism could serve as a potential signal.

Over 20 years ago, Berger suggested that massive, DNA damage causes an excessive activation of PARP-1 which, in turn, depletes NAD^+ pools within only a few minutes. Consequently, the main NAD^+-dependent metabolic pathways such as glycolysis and mitochondrial respiration are impaired, leading to reduced ATP production and cellular dysfunction. Moreover, under these precarious conditions phosphoribosyl pyrophosphate synthetase (PPS) and nicotinamide mononucleotide adenylyl transferase (NMAT) consume

ATP in an effort to resynthesize NAD^+, worsening the energetic shortage and contributing to the generation of a lethal, futile cycle. This cellular suicide mechanism has been implicated in the pathomechanisms of neurodegenerative disorders, cardiovascular dysfunction and various other forms of inflammation. Pharmacological inhibition or genetic ablation of PARP-1 significantly improved cellular energetic status and cell viability after exposure to necrosis-inducing agents.

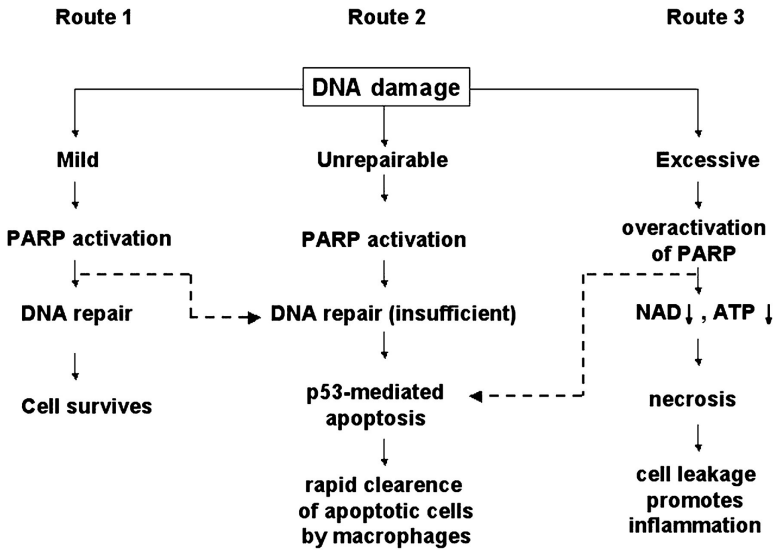

Figure 1. The intensity of DNA damaging stimuli determines the fate of cells: survival, apoptosis, or necrosis. In the case of mild DNA damage, poly(ADP-ribosyl)ation facilitates DNA repair and thus cell survival. (route 1). More severe genotoxic stimuli activate the p53 dependent (or independent) apoptotic pathway (route 2). The most severe DNA damage may cause excessive PARP activation, depleting cellular NAD^+/ATP stores leading to necrosis. (route 3). Pharmacological inhibition of PARP-1 in cells entering route1 inhibits repair and thus diverts cells to route 2 (broken arrow). The inhibition of PARP in cells route 3 preserves cellular energy stores and thus enables apoptotic machinery to operate (broken arrow) (Virag and Szabo, 2002)

1.3.3. PARP-1 in the transcription regulation and inflammation

PARP-1 has been shown to associate with and regulate the function of several transcription factors: Activating protein, AP-2, factor Yin Yang, YY1, Oct-1, transcription enhancer factor 1, TEF-1, B-MYB. Of special interest is the regulation of NF-κB-mediated transcription by PARP-1 bacause NF-κB and PARP-1 have both been demonstrated to play a pathophysiological role in a number of inflammatory disorders. The strongest indication for a direct role or PARP-1 and NF-κB dependent transcription was the impaired expression of NF-κB dependent pro-inflammatory mediators in PARP-$1^{-/-}$ mice.

Cytokines

Cytokines are substances that are secreted mainly by endo/epithelial cells and resident macrophages and which carry signals locally between cells, and thus have an effect on other cells. Cytokines act through cell surface receptor on the target cell subsequently initiate cascades of intracellular signaling then alter cell function. This may include the upregulation and/or downregulation of several genes and their transcription factors (e.g. NF-κB and/or AP-1), resulting in the production of other chemokines and other cytokines, an increase in the number of surface receptors for other molecules, or the suppression of their own effect by feedback inhibition. The cytokines tumor necrosis factor alpha (TNF-α) and interleukin beta (IL-1β) are key proinflammatory mediators. Both of them are potent inducers of chemokine production by many cell types including pulmonary epithelial cells. These chemokines, produced by airway epithelial cells, play a critical role in regulating local inflammatory processes in the lung.

Chemokines

Chemokines are 8-12 kDa, basic proteins that are the major mediators of all leukocyte migration. Their name is derived from their ability to induce directed chemotaxis in nearby responsive cells; they are chemotactic cytokines. There are nearly 50 distinct chemokines and 19 chemokine receptors. Inflammatory chemokines function mainly as chemo-attractants for leukocytes, recruiting monocytes, neutrophils and other effector cells from the blood to sites of infection or tissue damage.

Role of PARP-1 in inflammation

Many studies have demonstrated that PARP inhibitors selectively regulated the expression of cytokines and chemokines in inflammatory disease models. Defective iNOS expression both at the level protein and mRNA level in LPS and IFN-γ stimulated PARP-$1^{-/-}$ fibroblast cells was observed by Szabo (1998). Furthermore, PARP-1 inhibition reduced the expression of ICAM-1, P-selection, E-selectin and mucosal addressin cell adhesion molecule-1 in cytokine-stimulated human umbilical vein endothelial cells. Reduced expression of chemokines and adhesion molecules may be responsible for the reduced migration of inflammatory cells, the most common anti inflammatory effect of PARP inhibition as observed in animal studies (Zingarelli et al., 1998; Hasko et al., 2002). However it is not

known whether macrophages or parenchymal cells are the main targets of PARP inhibitors in these diseases. PARP-1 has also been implicated in the regulation of AP-1 driven transcriptional activity. Zingarelli's group reported alterations in AP-1 activation in oxidativelly stressed or IL-1 treated murine PARP-1 knockout fibroblast. They found decreased AP-1 DNA binding in PARP-$1^{-/-}$ cells after peroxynitrite, hydrogen peroxide or IL-1 stimuli. Furthermore, increased basal JNK activity and c-Jun phosphorylation were found accompany changes. (Andreone et al., 2003). Microarray analyses revealed that expression of several AP-1 dependent genes of proinflammatory mediators and heat shock proteins was altered in knockout animals. (Zingarelli et al., 2003).

De Murcia's group identified firstly deficient NF-κB activation as the underlying mechanism of the endotoxin resistance of PARP-$1^{-/-}$ mice. In TNFα treated fibroblast, IκB degradation and nuclear translocation of p65 was found unaltered in PARP-$1^{-/-}$ cell whereas DNA binding of p65 was markedly reduced. Thus was proposed that PARP-1 is required for NF-κB-mediated transactivation. (Oliver 1999). Chang and Alvarez-Gonzales found that non-poly(ADP-ribosyl)atad PARP-1 can bind to NF-κB-p50 + consensus oligonucleotide complex. Upon modification of PARP-1 the complex dissociated suggesting that PARP-1 enzyme activity regulated the interaction between the enzyme and the transcription factor. (Chang WJ, 2001). However, Hassa et al. have demonstrated that DNA binding and catalytic activity of PARP-1 is not required for the NF-κB coactivator function. They proposed that PARP-1 physically interacts with the Mediator complex, p300/CBP and with both subunits of NF-κB (p50 and p65), resulting in enhanced transactivation (Hassa et al., 2003).

We can conclude that the function of PARP-1 and poly(ADP-ribosyl)ation as a regulator of inflammatory signal transduction and transactivation shows marked cell-type and stimulus dependency.

2. AIMS OF THE STUDY

To investigate

- the effect of PARP-1 inhibitor PJ34, and a potent PARG inhibitor gallotannin on the TNFα-IL1β induced chemokine and cytokine gene-expression in A549 human lung epithelial cells, and
- role of PARP-1 and PARG proteins in hydrogen peroxide-induced cell death in A549 cells.

3. MATERIAL AND METHODS

3.1. Cell culture and treatments

All experiments involved A549, a human lung adenocarcinoma cell line representative of distal respiratory epithelium. The cell line was grown and maintained in a 5% CO_2 incubator at 37°C using RPMI-1640 containing 10% fetal bovine serum (FBS). Before TNFα and IL-1β treatment, cells were grown to confluency and incubated in serum-free medium for 12 hours. Where used, 10 μM PARP inhibitor PJ34 and the PARG inhibitor 30 μM gallotannin (GT) were added 30 min prior to stimulation by recombinant human TNF-α (20 ng/ml) and recombinant human IL-1β (5 ng/ml). Transformed human kidney cell line 293T was maintained in DMEM supplemented with 10% FBS at 37°C, 5% CO_2. Mesenhymal stem cells were isolated from umbilical cords and maintained in DMEM supplemented with 10% FBS at 37°C, 5% CO_2, after obtaining informed consent from donors. The protocol was approved by the Ethical Board of the Medical and Health Science Center of the University of Debrecen under permission no. 2754-2008.

3.2. Production of lentiviruses and infection of A549 cells

For shRNA-mediated stable knockdown, we employed a Mission Lentiviral-mediated gene specific shRNA system (Sigma). Short-hairpin RNAs (shRNAs) cloned into the lentivirus vector pLKO.1-puro were chosen from the human library (MISSION TRC-Hs 1.0) and purchased in bacterial glycerol stock form. pLKO.1-puro empty vector was used as a negative control. Lentiviral vectors were produced and used according to the manufacturer's protocol. The control shRNA and the shRNAs to PARP-1 and PARG were cotransfected with

the packaging plasmids into HEK293T cells to generate lentivirus particles using PEI as a transfection reagent. Infectious lentiviruses were harvested at 48 hours posttransfection and filtered through 0,45 μm nitrocellulose filters. Virus titers were determined by cell culture titration**.** After 24 hours transduced cells were selected and expanded in the presence of puromycin at final concentration of 5 μg/mL. Seven days later cells were fixed with 4% formaldehyde and subsequently stained with hemotoxilin for 20 min at room temperature. Cells were then washed with tapwater and air dried, colonies were counted and virus titers were calculated. The infection of A549 cells with control, shPARP-1 and shPARG lentivirus particles was carried out by addition of lentivirus into the cell culture with a multiplicity of infection of 10. Following transduction, virus-containing supernatant was removed after 24 hours and cells were selected with 5 μg/mL puromycin.

3.3. Macroarray

Profiles of TNFα/IL-1β-induced gene expression from A549 cells were determined by using the protocol of GEArray pathway-specific expression arrays from SuperArray. After treatment with TNFα and IL-1β for 4 hours, total RNA was isolated using SV Total RNA Isolation System (Promega) according to the manufacturer's instruction. Concentration and purity of the isolated RNA was measured spectrophotometrically at 260 nm and 280 nm. For the synthesis of cDNA probe, GEAprimer mix and reverse transcriptase primers were used. The resulting cDNA probes were hybridized to gene-specific cDNA fragments on the membranes. The relative expression level of each gene was determined by comparing the signal intensity of each gene in the array to the signal of housekeeping genes (β-actin, GAPDH).

3.4. RNA isolation and RT-PCR

Total RNA was isolated using TRIZOL (Applied Biosystems/Ambion) according to the manufacturer's instruction. Concentration and purity of the isolated RNA was measured spectrophotometrically at 260 nm and 280 nm, than 2 μg total RNA was reverse transcribed. PCR reactions for chemokine and cytokine mRNA-s were performed using RedTaq Polymerase (Sigma). PCR reactions for PARP-1 and PARG genes were performed using GoTaq Polymerase (Promega). Products were run on 1-2% agarose gel and visualized by ethidium bromide staining. PCR primers used for the analysis were designed based on sequences deposited in the UniGene database.

3.5. Real-time mRNA analysis

Two micrograms of total RNA was reverse transcribed as described above. Quantitative real-time PCR analysis was performed using an ABI PRISM 7500 sequence detector system (Applied Biosystems). Power SYBR Green PCR Master Mix reagents were purchased from Applied Biosystems and reactions were carried out according to the manufacturer's protocol in 25 μl total volume. The relative abundance of mRNAs was calculated by the comparative cycle of threshold (C_T) method with β-actin mRNA as the invariant control.

3.6. Nuclear extract preparation for EMSA analysis

Cells were washed with PBS and harvested by scraping into 1 ml of PBS and collected by centrifugation. The pellet was resuspended in hypotonic buffer „A" (10 mM HEPES pH 7.9, 10 mM KCl, 0.1 mM EDTA, 0.1 mM EGTA, 1 mM DTT, 0.5 mM PMSF, protease inhibitors) and allowed to swell on ice for 15 minutes. After adding Nonidet P-40 (NP-40) cells were vortexed than centrifuged. The pellet was resuspended in hypertonic buffer „B" (20 mM HEPES pH 7.9, 420 mM NaCl, 0.5 mM EDTA, 0.5 mM EGTA, 1mM DTT, 0.5 mM PMSF, protease inhibitors) and incubated on ice with occasional vortexing. Nuclear extracts were recovered after centrifugation for 10 min at 10,000 rpm. Protein concentrations were determined with Coomassie Plus Protein Assay reagent (Pierce Biotechnologie) and samples were stored at -70^{o}C until use for EMSA.

3.7. Electrophoretic mobility shift assay (EMSA)

The consensus NF-κB and AP-1 probes were obtained from Sigma. The probes were labeled with biotinylated ribonucleotides using Biotin 3'End DNA labeling kit (Pierce Biotechnologie Inc.) following the manufacturer's instruction. Gel shift assay was performed using a LightShift Chemiluminescent EMSA kit (Pierce Biotechnologie Inc.) following the manufacturer instructions. Briefly, protein-nucleic acid complexes were resolved using a non-denaturating polyacrylamide and run in 0.5x TBE for 1 h at constant voltage (100V). Gels were transferred to Bio Bond-Plus nylon membrane followed by DNA cross-linking using UV-light. Membrane was subsequently incubated in blocking solution (supplied by the LightShift kit) followed by labeling with streptavidin-peroxidase. After extensive washing, signal was detected with chemiluminescence solution (supplied with the kit).

3.8. Western blot analysis

20 μg protein was loaded per lane on an 10% SDS-polyacrylamide gel. For poly(ADP-ribose)polymer analysis, proteins were loaded on 8% SDS-polyacrylamide gel then separated electrophoretically and transferred to nitrocellulose membranes. Membranes were blocked with 5% non-fat dry milk in TBS-Tween20 (TBSTw). Primary antibodies were used at 1000 fold of dilutions overnight at 4°C. After extensive washing secondary antibodies (peroxidase-conjugated goat anti-mouse or anti-rabbit IgG), were used for 1 hour. Following extensive washing and incubating in chemiluminescent substrate membranes were exposed to photographic film.

3.9. Immunofluorescent staining

NF-κB p65 polyclonal antibody was used to monitor NF-κB nuclear translocation. Poly(ADP-ribose) was detected using monoclonal anti-poly(ADP-ribose) antibody. Cells were fixed in ice-cold 10% trichloroacetic acid (TCA), dehydrated by 70%, 90%, and 100% ethanol at -20°C. In case of NF-κB nuclear translocation, TCA treatment was omitted. Following rehydration with PBS, coverslips were blocked in horse serum diluted in PBS-Triton X-100 (PBSTx) for 1 hour and were then incubated overnight at 4°C with the first antibody. After washing, coverslips were incubated with biotinylated horse anti-mouse or anti-rabbit IgG. Incorporated biotin was detected by streptavidin-AlexaFluor-488 (Molecular Probes) diluted 1:100 in PBS. Coverslips mounted in antifade medium and viewed with a Zeiss Axiolab microscope. Pictures were taken with a Zeiss Axiocam digital camera.

3.10. Immunocytochemical detection of poly(ADP-ribose)

Monitoring the effect of shRNAs, cells were treated with hydrogen peroxide for different periods of time. Cells were then fixed in ice cold methanol for 10 minutes and hydrated by successive washes in PBS. Endogen peroxidase activity was eliminated by hydrogen peroxide treatment followed by washing with PBS. Coverslips were blocked in 1% BSA diluted in PBSTx for 1 hour and were then incubated anti-poli(ADP-ribose) antibody. After washing it with PBS, coverslips were incubated with biotinylated anti-mouse IgG. Excess antibody was removed by washing, and the bound antibody was visualized with the ABC detection system (Vector Laboratories) and 3,3'-diaminobenzidene substrate. Coverslips

were viewed with a Zeiss Axiolab microscope. Pictures were taken with a Zeiss Axiocam digital camera.

3.11. Phosphatase activity assay

The catalytic subunits of protein phosphatase 1 (PP1c) and 2A (PP2A) were prepared from rabbit skeletal muscle and the two types of phosphatase were separated by heparin-Sepharose chromatography. Phoshatases were incubated for 5 minutes with gallotannin at final concentrations of 0.5, 2, 10, 50 μM. The activity of PP1c and PP2A was determined with ^{32}P-labeled 20-kDa gizzard myosin light chain as substrate. Assays were performed at 30°C for 10 minutes, then the released $^{32}P_i$ was determined (after precipitation of proteins with 10% ice cold TCA and centrifugation 10,000g for 1 minute) from the supernatant in scintillation counter.

3.12. ABTS-assay

The antioxidant capacity was determined using the $ABTS^{\cdot}$ decolorisation assay. 2,2'-Azino-bis-(3-ethylbenzothiazoline-6-sulfonic acid) (ABTS) was used as a free radical provider and was generated by reacting this compound with potassium persulphate. The solution was diluted with Glycine-HCl to obtain an absorbance of 1.5 at 414 nm. An aliquot (140 μL) of the solution was added to 10 μL of sample into 96 well plate and the standard curve was prepared using similar volume of L-ascorbic acid. All readings were taken after 30 min of reaction time when the absorbance appeared to reach a plateau.

3.13. DHR-assay

Peroxynitrite scavenging effect was measured by monitoring the oxidation of dihydrorhodamine DHR123 using fluorescence spectrophotometer with excitation/emission wavelength of 485/527, at room temperature in the presence or absence of the test-compound.

3.14. Measurement of PARP activity

PARP activity assay based on the incorporation of isotope from ^{3}H-NAD^{+} into TCA-precipitable proteins. Medium was removed from the cells 20 min after hydrogen-peroxide treatment and cells were incubated at 37°C in 0.5 ml assay buffer (56 mM Hepes pH 7.5, 28 mM KCl, 28 mM NaCl, 2 mM $MgCl_2$, 0.01% digitonin, and 0.125 μM ^{3}H-NAD^{+}). Cells were collected and precipitated by ice-cold TCA for 4 h at 4°C. Samples were then spin down and

the pellets were washed in ice-cold 5% TCA and solubilized overnight in 250 µL 2% SDS/0.1 N NaOH at 37°C. The contents of the tubes were added to scintillation liquid and radioactivity was determined in a liquid scintillation counter.

3.15. Cell viability assay (MTT)

Cell viability was assessed by the colorimetric MTT assay. Briefly, cells were treated with hydrogen peroxide in a 96 well plate. 24 hours later MTT was added to the cells in final concentration 0.5 mg/ml and incubated for an additional hour. The medium was then aspirated and the formazan crystals were dissolved by the addition of 100 µl dimethylsulfoxide. Optical density was determined in a plate reader at 550 nm.

3.16. Intracellular NAD^+ measurement

Following hydrogen peroxide treatment, cells were extracted in 0.5 N $HClO_4$, neutralized with 3 M KOH/125 mM Gly-Gly buffer (pH 7.4), and centrifuged. Supernatants were mixed with a reaction medium containing 0.1 mM 3-[4,5-dimethylthiazol-2-yl]-2,5-diphenyl-tetrazolium bromide, 0.9 mM phenazine methosulfate, 13 U/ml alcohol dehydrogenase, 100 mM nicotinamide, and 5.7% ethanol in 61 mM Gly-Gly buffer (pH 7.4). Absorbance was determined in a plate reader at 560 nm immediately and after 10 min. NAD^+ levels were calculated from a standard curve generated with known concentration of NAD^+.

3.17. Assessment of intracellular ATP levels

To measure intracellular ATP levels, we used the luminometric ApoSENSOR Cell Viability Assay Kit (BioVision) according to the manufacturer's protocol. ATP drop was calculated as a percentage of untreated cell control. Assays were performed at 24 hours in three independent experiments.

3.18. Clonogenic assay

After treatment with hydrogen peroxide for 1 h at 37°C, cells were washed in order to remove hydrogen peroxide. Cells were further diluted in culture medium to get 10^2 up to 10^4 cells/ml and plated onto 6 well plates followed by culture at 37°C for 10 days. Cells were fixed with 4% formaldehyde then stained with hematoxilin for 10 min. After intensive washing with tap water, plates were air dried and colonies were counted.

3.19. Propidium-iodide uptake

Hydrogen peroxide-induced cytotoxicity was measured by propidium iodide uptake. After hydrogen peroxide treatment, cells were stained with 5 μg/mL propidium iodide solution for 15 min. Floating and adherent cells were then collected and centrifuged for 5 min at 2000 rpm, washed with PBS and analyzed by flow cytometry.

3.20. Measurement of caspase activation

Caspase-3-like activity was measured by the cleavage of the fluorogenic tetrapeptide-amino-4-methylcoumarine conjugate (DEVD-AMC). 24 hours after hydrogen peroxide exposure, floating and adherent cells were pooled and resuspended in lysis buffer. Cell lysates and substrates were combined in triplicate in the caspase reaction buffer and incubated for 1 hour at 37^{o}C. Fluorescence of released AMC has been measured by a microplate fluorimeter (Labsystems) at excitation wavelength of 380 nm and emission wavelength of 460 nm.

3.21. Detection of DNA fragmentation

Internucleosomal DNA fragmentation was quantitatively assayed by antibody-mediated capture and detection of cytoplasmic mononucleosome- and oligonucleosome-associated histone-DNA complexes (Cell Death Detection ELISA Plus, Roche Molecular Biochemicals). After treatment with hydrogen peroxide floating and adherent cells were pooled and resuspended in lysis buffer (supplied by the manufacturer) and incubated for 30 minutes at room temperature. After pelleting nuclei the supernatant (oligonucleosome-sized fragments derived form apoptotic cells) was used in the enzyme linked immunosorbent assay (ELISA) following the manufacturer's standard protocol. Finally, absorbance at 405 nm, upon incubation with a peroxidase substate was determined with a microplate reader.

3.22. Giemsa staining

Cells were seeded on glass coverslips for overnight. Following hydrogen peroxide treatment cells were washed with PBS, fixed with formalin then stained with May-Grünwald-Giemsa for 10 min. After intensive washing with tap water, coverslips were viewed with a Zeiss Axiolab microscope. Pictures were taken with a Zeiss Axiocam digital camera.

3.23. Analysis of mitochondrial membrane potencial

Cells were seeded on glass coverslips and cultured overnight before the experiment. Following hydrogen peroxide exposure, the coverslips were rinsed in phosphate-buffered

saline then cells were loaded with 1 μM JC-1 mitochondrial membrane potential-sensitive fluorescent dye for 30 min. Then the same microscopic field was imaged using a fluorescent microscope equipped with a digital camera first with red, then with green filters.

3.24. Comet assay

DNA single strand breaks were assayed by single cell gel electrophoresis. Broken DNA unwinds under alkaline conditions and forms comet-like structures after cell lysis and electrophoresis. Following hydrogen peroxide treatment cells were embedded into low melting point agarose and were layered onto the agarose-covered slides. After the agarose has cooled down, slides were placed into lysis solution. Following electrophoresis, slides were equilibrated and subsequently stained with ethidium bromide. Comets were analyzed by fluorescent microscopy.

3.25. Preparation of subcellular fractions of A459 cells

24 hours after hydrogen peroxide exposure, floating and adherent cells were pooled and washed with ice-cold PBS. Cells were diluted with four volumes of homogenization buffer (0.5 M sucrose, 20 mM HEPES, pH 7.5, 1 mM EDTA, 1 mM EGTA and protease inhibitors). The cell suspension was homogenized Dounce homogenizer in the presence of NP-40. The lysate was vortexed then microcentrifuged at 8000 x g at 4^{o}C. The pellet, containing the nuclei and cell debris, was resuspended in 3 volumes of buffer A (0.5 M sucrose, 10 mM HEPES, pH 7.9, 3.3 mM $MgCl_2$, 10 mM KCl, 0.5 mM DTT and protease inhibitors) and centrifuged. The supernatant was discarded and the pellet was resuspended in 2.5 volumes buffer B (buffer A except for 0.35 M sucrose). The suspension was centrifuged then the pellet was resuspended in buffer B and sonicated on ice to disrupt the nuclear structures; the sonicated suspension was used as the *nuclear fraction*. The $8000 \times g$ supernatant was used as *postnuclear fraction*. Protein concentrations were determinated using BCA method. Fractions were subsequently analysed by Western blot.

Statistical analysis

All experiments were preformed three times on different days. Student's *t*-test was applied for statistical analysis and for the determination of significance with $p < 0.05$ considered as significant.

4. RESULTS AND DISCUSSION

4.1. GT significantly reduced the chemokine and cytokine gene expression in immunostimulated A549

We have used a nylon-based thematic low density array to investigate the effects of GT and PJ34 on the expression pattern of chemokines and inflammatory cytokines in A549 cells. TNFα/IL-1β treatment significantly (minimum 2-fold induction) induced the expression of 12 genes (CXCR4, IL-1α, IL-1β, IL-6, MCP-1, MIP-3α, MIP-1β, RANTES, MCP-2, ENA-78, GCP-2, Fracalkine) and suppressed the expression of two cytokine receptor genes (CCR4, CCR5). Pretreatment of cells with gallotannin significantly reduced these alterations with the exception of one chemokine (MIP-3α). PJ34 significantly enhanced fractalkine expression. To confirm our results, we also carried out RT-PCR reactions for seven genes; each reaction gave similar results. In addition, the expression of IL-8, a key neutrophil-recruiting chemokine that was not represented on the array, was also investigated with RT-PCR and found to be inhibited by both GT and PJ34.

4.2. GT and PJ34 decreased NF-κB activation but different manner

Because NF-κB and AP-1 are known to regulate the expression of various inflammatory cytokines and chemokines, we have investigated the effects of GT and PJ34 on the activation of these transcription factors. Treatment of A549 cells with TNFα/IL-1β induced NF-κB activation as demonstrated by EMSA analysis. Pretreatment of the cells with PJ34 or GT markedly reduced the binding of NF-κB to its consensus oligonucleotide. TNFα/IL-1β-induced nuclear translocation of NF-κB was blocked by GT but was unaffected by PJ34, indicating that PARP inhibition by PJ34 may inhibit the DNA binding of the transcription factor. As for GT, we have also investigated IκB phosphorylation, an event laying upstream in the NF-κB pathway. GT abolished phosphorylation, suggesting that GT may inhibit the kinase cascade (IκB kinase or upstream kinases).

4.3. GT enhanced JNK-c-Jun-AP-1 pathway but inhibited AP-1 transactivity

We have observed a basal AP-1 activity as demonstrated by EMSA experiments. TNFα/IL-1β treatment triggered further AP-1 activation. GT pretreatment abolished both basal and TNFα/IL-1β-induced AP-1 activation while PJ34 had no effect on AP-1 activation. Mitogen-activated protein kinases JNK, p38MAPK, and ERK1/2 play key roles in cytokine-

induced signaling. TNFα/IL-1β induced a rapid phosphorylation of JNK and c-Jun. Surprising GT stimulated basal JNK phosphorylation that was not further increased by the cytokines. GT also induced maximal c-Jun phosphorylation that was not further enhanced by TNFα/IL-1β. PJ34 had neither effect on JNK phosphorylation nor on c-Jun phosphorylation. c-Jun can heterodimerize with ATF2 that is regulated mainly by p38MAPK. Therefore, we also determined whether GT and PJ34 affect the p38MAPK-ATF2 pathway. TNFα/IL-1β induced a rapid phosphorylation of p38MAPK which was not affect by PJ34. However, GT alone caused a low-level phosphorylation of p38MAPK. The TNFα/IL-1β-induced signal was slightly reduced by GT. Phosphorylation of ATF2 was similarly affected by the two drugs with no effect of PJ34 and inhibition of cytokine-induced ATF2 phosphorylation by GT. We found that ERK1/2 and CREB are regulated by GT the same way as seen with p38MAPK and ATF2. Whereas PJ34 had no effect on the basal and cytokine-induced phosphorylation of ERK1/2 and CREB, GT induced the phosphorylation of these proteins but inhibited their further activation by cytokines.

4.4. GT inhibits protein phosphatases

Considering that GT increased the phosphorylation state of many proteins (JNK, c-Jun, p38MAPK, ATF2, ERK1/2, and CREB), we hypothesized that GT may interfere with the activity of protein phosphatases. We have determined the effect of GT on the activities of protein phosphatases 1 and 2A and found that GT inhibited both phosphatases in a concentration-dependent manner.

4.5. GT has no affect on poly(ADP-ribose) metabolism in our model

We also sought to determine whether the transcriptional regulatory effect of GT is related to PARG inhibition. Treatment of cells with GT in the absence or presence of the cytokines caused no elevation in the cellular poly(ADP-ribose) content. The lack of poly(ADP-ribose) accumulation in GT-treated cells suggest that no major alterations of poly(ADP-ribose) metabolism occur in response to GT treatment. Treatment of the cells with the cytokines for various time periods caused no elevation in cellular poly(ADP-ribose) content as determined by immunofluorescence or Western blotting.

It seems unlikely that PARG is the major target of GT in our system. Nonetheless, poly(ADP-ribose) accumulation on certain low abundance proteins may remain undetected in Western blots or immunofluorescent stainings and may be important for the regulation of transcription

4.5. GT has a strong antioxidant activity

Another feature that could, at least in part, explain the effect of gallotannin on cytokine/chemokine expression is the well known antioxidant effect of tannins. Considering that both NF-κB and AP-1 are redox-sensitive transcription factors modification of the cellular redox state by GT could be responsible for the described effect of GT. We have studied the radical-scavenging effect of GT and PJ34 in the ABTS decolorization assay. In this assay, GT displayed an even more potent radical-scavenging effect compared with the well known antioxidant ascorbic acid. However, PJ34 did not scavenge the radical. We have also used the pathophysiologically relevant oxidant peroxynitrite. Peroxynitrite oxidizes DHR123 into fluorescent rhodamine. The addition of GT and ascorbic acid inhibited peroxynitrite-induced DHR123 oxidation, with GT being the more potent antioxidant. PJ34 had no effect.

4.6. We established and characterized A549 cell lines with stably suppressed hPARG and hPARP1

We have generated cell lines with suppressed expression of PARG and PARP-1. For stable silencing lentiviral particles were used. The efficiency of the gene silencing was confirmed by reverse transcription-coupled PCR and real-time quantitative PCR. Knockdown of PARP-1, at protein level, has also been established by Western blotting. Expression of PARG protein was not detected because of the lack of available antibody. However, functional characterization of the shPARG cell line, as shown, proved the efficient suppression of PARG protein levels.

4.7. shPARG cells exhibit delayed poly(ADP-ribose) catabolism after hydrogen peroxide treatment

To further characterize our cell lines and to learn how knockdown of PARG and PARP-1 affects poly(ADP-ribose) metabolism, the cell lines were subjected to functional characterization. In A549 cells, hydrogen peroxide treatment caused transient nuclear synthesis of poly(ADP-ribose), as assessed by immunocytochemical analysis using a

polymer-specific antibody. The polymer level was restored within 15 min in A549 and cells infected with control lentiviruses. In the shPARP-1 cell line, however, poly(ADP-ribose) synthesis was strongly suppressed. Poly(ADP-ribose) synthesis was apparently unchanged in shPARG cells; however, degradation of the polymer was significantly delayed, with no obvious sign of poly(ADP-ribose) degradation at 15 min and strong immunopositivity detected even 120 min after hydrogen peroxide treatment. Altered poly(ADP-ribose) metabolism has also been confirmed in Western blot experiments.

These data clearly demonstrate that efficient suppression of the main poly(ADP-ribose) synthesizing and degrading enzyme has been achieved in A549 cells.

PARP activity was determined by ^{3}H-NAD incorporation in unstimulated and hydrogen peroxide-treated cells. Both basal and hydrogen peroxide-induced PARP activity was reduced in the shPARP-1 cell line. Knockdown of PARG had no effect on basal PARP activity, whereas hydrogen peroxide-induced PARP activity was significantly reduced. These data indicate that by removing inhibitory poly(ADP-ribose) polymers from PARP-1, PARG permits constantly high PARP-1 activity in oxidatively stressed cells.

4.8. shPARP-1 and shPARG cells are resistant to hydrogen peroxide induced cell death

Hydrogen peroxide caused a concentration-dependent decrease in the viability of control A549 cells. shPARG and shPARP-1 cells were significantly protected from toxicity of the oxidant, with PARG knockdown providing weaker protection. Similar patterns could be observed in the drop of cellular NAD^+ and ATP levels indicating that compromised cellular energetics could explain the PARP/PARG-dependent component of hydrogen peroxide-induced cytotoxicity. Indeed, TCA-cycle substrates methyl pyruvate and ketoglutarate provided significant protection from hydrogen peroxide-induced cell death, indicating that slowdown of glycolysis contributes to loss of viability in this model. Inhibition of glycolysis may result in mitochondrial depolarization, an event mediated by PARP activation in cells exposed to DNA damage. In our model, hydrogen peroxide triggered a concentration-dependent mitochondrial depolarization that was blocked in shPARP-1 and shPARG cells. In shPARG cells this could be explained with the longer maintenance of the auto-inhibited PARP-1.

4.9. Concerted action of PARG and PARP-1 mediates apoptosis to necrosis switch in severe oxidative stress

To further characterize the mode of cell death in our model, we have determined plasma membrane permeability. Exposure of cells to high concentrations of hydrogen peroxide lead to increased plasma membrane permeability, as indicated by propidium iodide uptake. Loss of plasma membrane integrity is mediated by the activation of PARP-1, as shPARP-1 cells were resistant to hydrogen peroxide-induced plasma membrane permeabilization. PARG may also contribute to the permeabilization of the plasma membrane, as shPARG cells were, although to a lesser extent, also protected from the loss of plasma membrane integrity.

4.10. Caspase-dependent and AIF independent apoptosis is prolonged in shPARP-1 and shPARG cells

Apoptotic parameters such as caspase-3-like activity and internucleosomal DNA fragmentation declined at higher concentrations of the oxidant. However, in shPARP-1 cells and, to a lesser extent, in shPARG cells, these apoptotic parameters were significantly more preserved, indicating that a concerted action of PARP-1 and PARG is required for the apoptosis-to-necrosis switch in oxidatively stressed A549 cells. Interestingly, shPARG cells seemed to be more sensitive to lower concentration of oxidant. Indeed, they exhibited higher caspase-activity and increased DNA fragmentation at lower hydrogen peroxide concentration. We also show that DNA fragmentation is caspase-dependent in our model because DNA fragmentation could be abolished by the pancaspase inhibitor zVAD-fmk.

As AIF release has been proposed to propagate poly(ADP-ribose) mediated cell death, we sought to determine AIF relocation following hydrogen peroxide treatment. In untreated cells, AIF exhibited a punctuate distribution in the cytoplasm, corresponding to the mitochondrial localization of the protein. Hydrogen peroxide failed to induce AIF translocation from the mitochondria to the nucleus, indicating that AIF is not likely to mediate cell death in our model. Lack of nuclear translocation of AIF in A549 cells could also be confirmed in subcellular fractionation experiments. Cells were fractionated into nuclear and postnuclear fractions, and AIF was detected with Western blotting.

Suppression of PARG expression decreased necrosis (as assessed by membrane permeability and ATP measurements) and led to increased apoptotic parameters, such as caspase-3-like activity and oligonucleosomal DNA fragmentation. These data indicate that PARG, similarly to PARP-1, mediates apoptosis-to-necrosis switch in severe oxidative stress. According to this scenario, PARG suppression leads to increased automodification of PARP-1, which is known to lead to PARP-1 autoinhibition. In support of this, the major band of

poly(ADP-ribose)-modified proteins in untreated shPARG cells corresponds to the size of PARP-1. Furthermore, PARG knockdown resulted in reduced PARP activation in hydrogen peroxide-treated cells, suggesting that auto-poly(ADP-ribosyl)ation indeed down-regulates PARP-1 activity.

4.11. Concerted action of PARG and PARP1 is required for the repair of oxidative stress-induced DNA breaks

One of the best-described biological functions of poly(ADP-ribosyl)ation is to assist DNA repair. Hydrogen peroxide induced a concentration-dependent DNA breakage as assessed in single-cell gel electrophoresis (comet assay). At 400 μM of hydrogen peroxide, massive DNA breakage could be observed. Considering the severity of DNA damage, cells coped remarkably well with the repair of DNA breaks, as shown by images obtained during the recovery phase. As an almost complete repair of damage could be observed at 45 min following hydrogen peroxide treatment, we compared the repair capacity of our cell lines at this time point. We observed an impaired DNA strand break repair in shPARP-1 cells and an almost complete blockage of repair in shPARG cells. Compromised DNA single-strand break repair may result in limited long-term clonogenic survival of shPARG and shPARP1 cells. Indeed, we determined clonogenic survival following treatment with 200 μM hydrogen peroxide, and both knockdown cells exhibited impaired clonogenicity.

5. CONCLUSION

1. TNFα/IL1β induces chemokine and cytokine gene-expression through NF-κB and AP-1 activation in A549 cells which is strongly suppressed by GT and weakly inhibited by the PARP-1 specific inhibitor PJ34.

2. GT decreased NF-κB transactivation by inhibiting its nuclear translocation. This effect is due to the inhibition of IκB phosphorylation. PJ34 did not affect the nuclear translocation of the transcription factor, however it inhibited its DNA binding.

3. GT also inhibited the DNA binding of the transcription factor, AP-1 even in the absence of cytokines. However, GT did not inhibit the activation of the AP-1 subunits. Moreover, we observed an elevated phosphorylation of c-Jun.

4. GT alone induced phosphorylation of JNK, p38MAPK and ERK1/2 and their targets. This might be due to the inhibition of protein phosphatases.

5. Lack of poly(ADP-ribose) accumulation in GT-treated cells suggests that no major alteration of poly(ADP-ribose) metabolism occur in response to GT treatment. Moreover, the cytokine exposure stimulated no detectable poly(ADP-ribose) synthesis in either the absence or presence of GT.

6. Stable gene silencing of PARG provided protection from hydrogen peroxide-induced loss of viability; however, the degree of protection was less than that observed in shPARP-1 cells.

7. Increased short-term viability of hydrogen peroxide treated shPARG cells, however, did not translate to increased long-term clonogenic survival.

8. PARG deficiency led to enhanced sensitivity against mild DNA damage.

9. Hydrogen peroxide-induced apoptosis seemed to be caspase-dependent and AIF independent in A549 cells.

10. Deficient repair of oxidative DNA breaks was observed both in shPARP-1 and especially in shPARG cells.

6. PUBLICATIONS

This thesis is built on the following publications:

Erdélyi K, Bakondi E, Gergely P, Szabó C, Virág L: Pathophysiologic role of oxidative stess-induced poly(ADP-ribose) polymerase-1 activation: focus on the cell death and transcriptional regulation. *Cell. Mol. Life Sci*. **62**(7-8):751-9. Review
IF: 4,812

Erdélyi K, Kiss A, Bakondi E, Bai P, Szabó C, Gergely P, Erdődi F, Virág L: Gallotannin inhibits the expression of chemokines and inflammatory cytokines in A549 cells. *Mol Pharmacol.* **68**(3):895-904. (2005)
IF: 5,080

Erdélyi K, Bai P, Kovács I, Szabó É, Mocsár G, Kakuk A, Szabó Cs, Gergely P, Virág L: Dual role of poly(ADP-ribose) glycohydrolase in the regulation of cell death in oxidatively stressed A549 cells. *FASEB J.* **23**(10):3553-63. (2009)
IF: 7.049

Other publications:

Bakondi E, Bai P, **Erdélyi K**, Szabó C, Gergely P, Virág L: Cytoprotective effect of gallotannin in oxidatively stressed HaCaT keratinocytes: the role of poly(ADP-ribose) metabolism. *Exp Dermatol.* **13** (3):170-8. (2004)
IF: 2,040

Zákány R, Bakondi E, Juhász T, Matta C, Szijgyártó Z, **Erdélyi K**, Szabó E, Modis L, Virag L, Gergely P: Oxidative stress-induced poly(ADP-ribosyl)ation in chick limb bud-derived chondrocytes. *Int J Mol Med*. **19**(4):597-605. (2007)
IF: 1,847

Bai P, Hegedűs C, **Erdélyi K**, Szabó E, Bakondi E, Gergely S, Szabó C, Virág L: Protein tyrosine nitration and poly(ADP-ribose) polymerase activation in N-methyl-N-nitro-N-nitrosoguanidine-treated thymocytes: Implication for cytotoxicity.
Toxicol Lett. **15**;170(3):203-13. (2007)
IF: 2,826

Posters:

Erdélyi K, Gergely P, Virág L:A poli-ADP-riboziláció szerepe A549 tüdőepitélsejtek gyulladásos kemokin- és citokinexpressziójának vizsgálatában. *Magyar Biokémiai Egyesület, Molekuláris Biológiai Szakosztálya 9. Munkaértekezlete* Sopron (2004)

Erdélyi K, Bak I, Bakondi E, Dinya Z, Antus S, Tósaki Á, Gergely P, Virág L: Characterization of the antioxidant, cytoprotective and cardioprotective effect of cherry, blackberry and sour cherry tannins. *Free radicals and diseases: gene expression, cellular metabolism and pathophysiology, International Free Radical Summer School* Spetses (2004)

Bakondi E, **Erdélyi K**, Gergely P, Virág L: Gallotannin regulates poly(ADP-ribose) metabolism and protects against cytotoxicity in oxidatively stressed HaCaT keratinocyte cells. *Free radicals and diseases: gene expression, cellular metabolism and pathophysiology, International Free Radical Summer School* Spetses (2004)

Bai P, **Erdélyi K**, Bakondi E, Hegedűs C, Gergely P, Szabó C, Virág L: The possible role of peroxynitrite production in the N-methyl-N-nitro-N-nitrosoguanidine (MNNG) induced cytotoxicity. *Peroxinitrite 04'* Konstanz (2004)

Erdélyi K, Bakondi E, Szabó C, Gergely P, Virág L: Suppression of chemokine and inflammatory cytokine expression by gallotannin in A549 cells is not related to inhibition of poly(ADP-ribose) glycohydrolase. *30th FEBS Congress and 9th IUBMB Conference* Budapest (2005)

Erdélyi K, Gergely P, Virág L: A poly(ADP-ribóz) glikohidroláz siRNS-sel történő gátlásának következményei A549 sejtekben. *Magyar Biokémiai Egyesület, Molekuláris Biológiai Szakosztálya 10. Munkaértekezlete* Pécs (2006)

Erdélyi K, Gergely P, Virág L: A poli(ADP-ribóz) szerepének vizsgálata a sejthalálban**.** *Genetikai és fejlődésbiológiai napok* Balatonfüred (2007)

Erdélyi K, Bai P, Hegedűs C, Gergely P, Virág L: Poli(ADP-ribóz) polimerek és a poli(ADP-ribóz)glikohidroláz sejthalálban való lehetséges szerepének vizsgálata A549

sejtekben. *Magyar Biokémiai Egyesület, Molekuláris Biológiai Szakosztálya 11. Munkaértekezlete*, Szeged (2008)

Presentations:

Bai P, **Erdélyi K**, Bakondi E, Hegedűs C, Gergely P, Szabó C, Virág L: Potential role of peroxynitrite in the poly(ADP-ribose) polymerase-mediated cytotoxicity caused by the alkylating agent N-methyl-N-nitro-N-nitrosoguanidine in thymocytes. *Poly-ADP-ribosylation in Health and Disease, FEBS Advanced Course* Debrecen (2003)

Erdélyi K: A poli-ADP- riboziláció szerepe A549 tüdőepitélsejtek gyulladásos citokin- és kemokinexpressziójának szabályozásában. *PhD és TDK Tudományos Diáktalálkozója* Debrecen (2004)

Bai P, **Erdélyi K**, Bakondi E, Hegedűs C, Gergely P, Szabó C, Virág L: Peroxinitrit lehetséges szerepe az N-metil-N-nitro-N-nitrozoguanin (MNNG) kiváltotta citotoxicitásban. *Magyar Biokémiai Egyesület Jelátviteli Konferenciája,* Sopron (2004)

Erdélyi K: A gallotannin hatása A549 sejtek gyulladásos citokin és kemokin expressziójára. *PhD és TDK Tudományos Diáktalálkozója,* Debrecen (2005)

Erdélyi K, Bai P, Kovács I, Gergely P, Virág L: A poli(ADP-ribóz) polimeráz-1 (PARP1) és a poli(ADP-ribóz) glikohidroláz (PARG) szerepének vizsgálata A549 sejtekben lentivirális géncsendesítéssel. *Membrán-transzport konferencia* Sümeg (2008)